

# Microstructure, Properties and Fracture Mechanism of Al 2014 Reinforced with Alumina Particles

M.N. MAZLEE AND J.B. SHAMSUL

*School of Materials Engineering*

*Northern Malaysia University College of Engineering (KUKUM) Jejawi, 02600 Arau, Perlis*

---

## ABSTRACT

*The studies of microstructure, properties and fracture mechanism have been conducted on Al 2014 matrix alloy reinforced with 10 volume percent (Composite 1) and 15 volume percent (Composite 2) of alumina ( $Al_2O_3$ ) particles respectively. Microstructure observation of the composite specimens was focused on the distribution of alumina reinforcement particles in different orientations. It was found that Composite 1 showed a more evenly distributed particles compared to that of Composite 2. The measurement of sonic modulus was carried out by using GrindoSonic MK5 Industrial Instrument. All the sonic modulus properties (flexural, longitudinal and torsional moduli) of Composite 2 were found to be higher than Composite 1. The testing of impact strength was done by means of Charpy impact test (V-notched specimen). It has found that the impact strength of Composite 1 (5.42 J) was higher as compared to Composite 2 (4.07 J). The fracture surfaces after impact test for the composite samples were investigated by using scanning electron microscopy in order to characterise the fracture mechanism of the composites. The fracture mechanism of Composite 1 was indicated by matrix ductile rupture and decohesion of particle-matrix interface, whereas matrix brittle rupture by particle fracture was found in Composite 2.*

**Keywords:** Al 2014, alumina, microstructure, sonic modulus, impact test, decohesion, particle fracture.

---

## INTRODUCTION

Aluminium matrix composites (AMCs) have become the most potential materials that have been used for the novel applications in aerospace and automotive industries due to its properties namely high specific strength, good wear resistance and low density. Microstructure of the composite material plays a very important role in determining the performance of the engineering components. One of the most important aspects of the microstructure is the distribution of the reinforcement particles and this depends on the processing and fabrication routes involved <sup>(1)</sup>. Microstructure of AMCs that have been investigated by other researchers include Al 2014/SiC <sup>(2)</sup>, Al/ $Al_2O_3$  <sup>(3-4)</sup>, Al-5% Si-0.2% Mg/SiC <sup>(5)</sup> and Al 7075/SiC <sup>(6)</sup>.

The reinforcement particles can also modify other aspect of the matrix microstructure such as deformation behaviour <sup>(7-9)</sup> and fracture mechanism <sup>(8, 10)</sup> of the composites. The relationship between microstructure and property is of technical importance for the

composite industries since there is direct effect between materials processing and materials behaviour to suit with the appropriate engineering applications.

Most of the studies on fracture mechanism of aluminium matrix composites were focused on the fractography resulted from fracture toughness test <sup>(11-12)</sup> and bending test <sup>(13-14)</sup>. However, very few studies on impact fractography resulted from sudden applied load of AMCs has been done <sup>(15)</sup>.

Most of the works reported were based on the elastic modulus of the metal matrix composites (MMCs) <sup>(16-18)</sup>. The study focused on sonic modulus instead of static measurement via elastic portion of the tensile stress-strain curve to measure the elastic modulus of the materials which had been conducted by Cemal Aksel and Frank L. Riley <sup>(19)</sup> on ceramic matrix composite. Thus, the objective of this research is to study the microstructure, properties and fracture mechanism of Al 2014 reinforced with Al<sub>2</sub>O<sub>3</sub> particles.

## METHODOLOGY

The materials used were Al 2014 (Al-Cu) matrix alloy reinforced with 10 vol. % (Composite 1) and 15 vol. % (Composite 2) of Al<sub>2</sub>O<sub>3</sub> particles. The particles size for both composites range from 9 to 13 µm. Both composites were produced by casting method followed by hot extrusion process. Composite 1 was in the form of rounded bar with 19 mm diameter and Composite 2 was in the form of rectangular bar with 77 mm wide and 19 mm thickness. The materials were supplied by Duralcan Inc., San Diego, California, USA.

Optical microscope was used to identify and analyse the microstructure of Composite 1 and Composite 2. The specimens were cut into small pieces and then mounted using hot mounting technique. Then the specimens were ground by wet grinding technique using silicon carbide papers (240, 400, 600, 1000, 1200 grit). Keller's reagent was used as an etchant to reveal the microstructure of the composites.

The sonic modulus test was carried out based on the impulse excitation technique. Samples machined to 10 x 10 x 55 mm dimension were taken for flexural, longitudinal and torsional moduli inspection before impact test was carried out as shown in Figure 1. Moduli were measured in longitudinal (L) orientation only for Composite 1 (Figure 2). For Composite 2, the moduli were measured in two orientations namely short-transverse (S-T) and longitudinal (L) orientation (Figure 3). The impact test was carried out using Charpy technique. The fracture surfaces of the composites after impact test were characterised by using scanning electron microscopy (Cambridge 200 model).

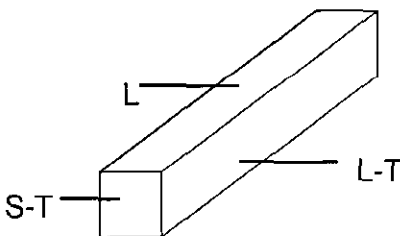
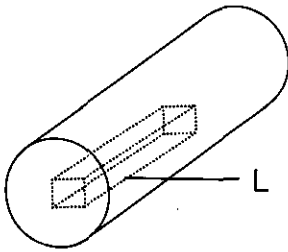
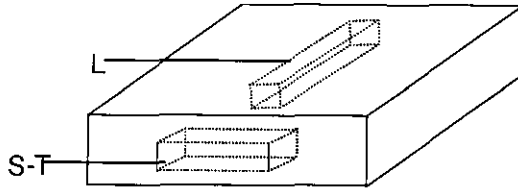


Figure 1: L, S-T and L-T orientations in the composites.



**Figure 2** L specimen orientations in Composite 1



**Figure 3:** L and S-T specimen orientations in Composite 2.

## RESULTS AND DISCUSSION

### Microstructure

Microstructure investigations of the composite specimens were focused on the distribution of alumina reinforcement particles in different orientations. Generally, the microstructures of the composites showed that the  $Al_2O_3$  particles were evenly distributed in the Al 2014 matrix alloy. However, it is found that Composite 1 shows more evenly distributed  $Al_2O_3$  particles compared to that of Composite 2 as shown in Figure 5.

Figures 4, to 8 indicate black phase as  $Al_2O_3$  particles meanwhile bright phase is the Al 2014 matrix alloy. A typical microstructure of the composite in the extruded state is shown in Figure 4. Figure 4 shows that some  $Al_2O_3$  particles clustering and some particles are oriented into or parallel to the extrusion direction synonym with a study of cast and hot extruded Al-5% Si-0.2% Mg reinforced with SiC particles<sup>(5)</sup>.

An optical micrograph of Composite 1 in S-T direction is shown in Figure 5. It shows that a more uniformly  $Al_2O_3$  particles distribution with no particle clustering in the Al 2014 matrix. The evenly distributed of the  $Al_2O_3$  particles may be due to the uniformly distributed applied pressure to the rounded sample of the Composite 1.

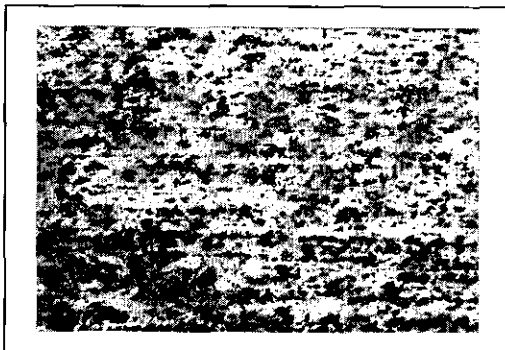


**Figure 4:** Optical micrograph of Composite 1 specimen in L direction (100 x).

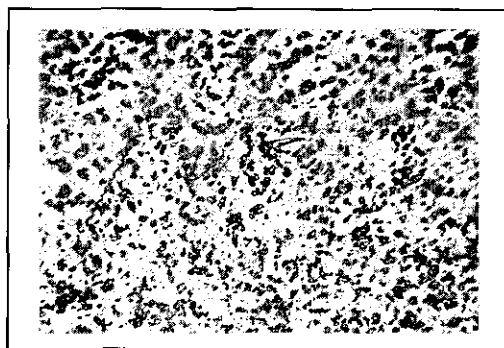


**Figure 5:** Optical micrograph of Composite 1 specimen in S-T direction (100 x).

**Figure 6**, shows the microstructure of Composite 2 in L direction. The  $Al_2O_3$  particles are uniformly distributed and some are realigned to the extrusion direction throughout the matrix. Less of  $Al_2O_3$  particles alignment to the extrusion direction may be due to the less distributed applied pressure during extrusion process due to the rectangular shape of the Composite 2. The  $Al_2O_3$  particles are not uniformly distributed in the Composite 2 in S-T direction as indicated in Figure 7.

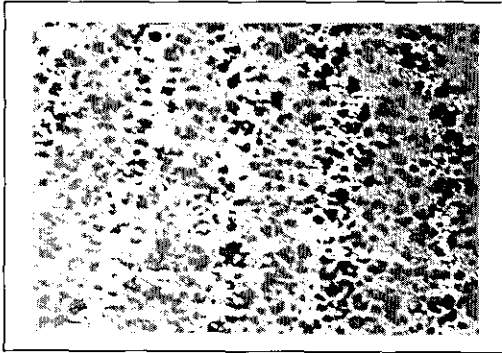


**Figure 6:** Optical micrograph of Composite 2 specimen in L direction (100 x).

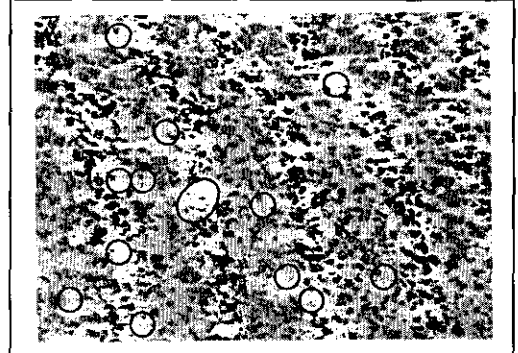


**Figure 7:** Optical micrograph of Composite 2 specimen in S-T direction (100 x).

The rounded blue lines show the areas that are not uniformly distributed by  $Al_2O_3$  particles.

Figure 8 shows the optical micrograph of Composite 2 in L-T direction. Less segregation of  $Al_2O_3$  particles are shown in the direction of extrusion process. However, the clustering and fragmentation of  $Al_2O_3$  particles are observed in the extrusion direction. The deformation banded structure is observed in Composite 2 as showed in Figure 7. It shows a very fine banded structure in between the  $Al_2O_3$  particles. The deformation banded structure appears to be in the extrusion direction may be due to the orientation of  $Al_2O_3$  particles in accompanied with the thermal mismatch between  $Al_2O_3$  particles and Al 2014 matrix alloy during hot extrusion process. Similar result is found in the aluminium matrix composite made by blending together the SiC and inert gas atomised aluminium powder followed by hot isostatic pressing <sup>(7)</sup>.

Figure 10 shows a schematic diagram for both features of the deformation banded structure namely rotated zone (Z) and distorted zone (R). In addition to the formation of deformation zones, large particles are also likely to disturb the slip pattern in the matrix resulting in a lensoid distortion of the slip plane and substructure around the particle as observed by F.J. Humphrey <sup>(7)</sup>. The formation of deformation zones may increase the modulus properties of the Composite 2 in longitudinal (L) direction as shown in Table 1.



Figure 8: Optical micrograph of Composite 2 specimen in L-T direction (100 x).

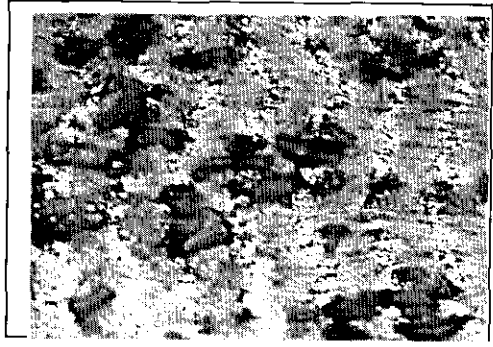


Figure 9: Optical micrograph of Composite 2 (500 x) in L-T direction shows the deformation banded structure indicated by D.

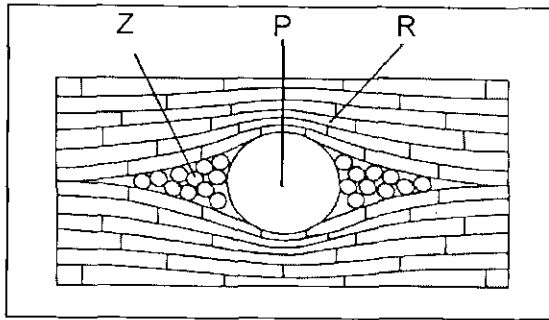


Figure 10: Schematic diagram should show the rotated deformation zones and the distortions associated with large particles (7); Z, P and R indicate a rotated zone, a particle and a distorted zone respectively.

### Sonic Modulus and Impact Test

Table 1, shows the results of sonic moduli and impact test. For sonic moduli, Composite 2 indicated higher average moduli in both orientations (L and S-T) compared to Composite

1. The elastic modulus was increased by the addition of reinforcement particles (1). This result was attributed to the higher volume percent of the reinforcement particles content. The improvement in modulus properties was observed follows the rule of mixture. Both values of flexural modulus of Composites 1 and 2 are found to be higher than static measurement via elastic portion of the tensile stress-strain curve which are 84 GPa and 92 GPa respectively as investigated by D.J. Lloyd (1) on the same composites.

Besides that, orientation of the direction also plays an important role in determining the effect on results of sonic moduli. From the results in Table 1, it is found that sonic moduli of the Composite 2 were higher in L direction compared to the S-T direction. This result is caused by the alignment of reinforcement particles in longitudinal direction during the extrusion process which contributes to the parallel distribution of particles. It is also found

that the results of sonic moduli and impact test have a significant relation whereas the composite with a higher value of sonic modulus will have a lower value of impact strength. An average value of impact strength of Composite 2 is lower than Composite 1. This condition is due to the adverse effect on toughness and ductility that is induced by reinforcement addition <sup>(20)</sup>.

**Table 1: Results of sonic moduli and impact test.**

Composite	Direction	Average Modulus (GPa)			Average impact energy (J)
		Flexural	Longitudinal	Torsional	
Composite 1	L	85.79	9.86	11.34	5.42
Composite 2	L	93.88	10.89	12.69	4.07
	S-T	95.34	10.81	12.54	4.07

**Fractography**

Figures 11 and 12 show the fractography of Composites 1 and 2 respectively after impact test. Figure 11 shows deep dimple morphology, plastic deformations in the matrix and decohesion at the particle-matrix interface which have a relation with a higher value of impact strength in Composite 1. In contrast to the observation in the forged composites <sup>(21)</sup>, no decohesion of SiC particles was observed after the extrusion process and fragmented particles were well covered by the matrix.

Meanwhile Figure 12 shows fracture and cleavage at reinforcement particle and cracking at the intermetallic inclusion at the surrounding of  $Al_2O_3$  particles. The existing cracks at particles then propagate simultaneously when the external energy in impact form is applied. The intermetallic inclusion (white coloured phase) at the surrounding of reinforcement particles will decrease the cohesiveness bonding between particle and matrix thus interface bonding will be further weaken.

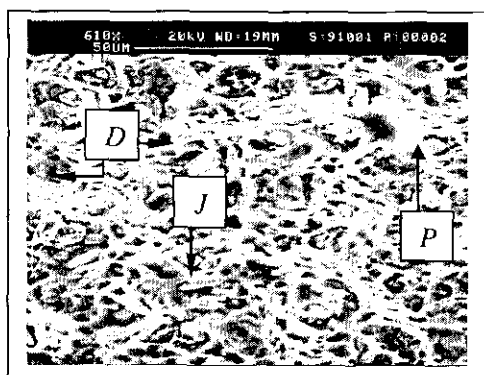


**Figure 11:** Fractography of Composite 1 shows the deep dimples morphology (D), plastic deformations in the matrix (P) and decohesion phenomenon at the particle-matrix interface (J).

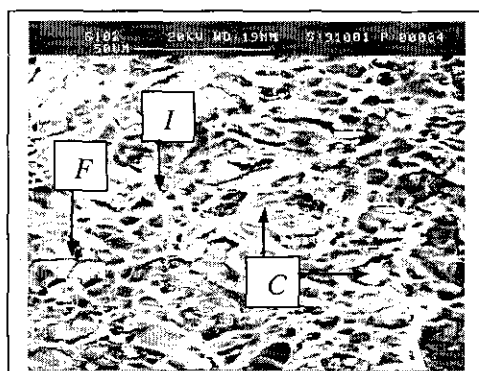


**Figure12:** Fractography of Composite 2 shows fracture of  $Al_2O_3$  particle (F), cleavage at  $Al_2O_3$  particle (C) and intermetallic inclusion at the surrounding of  $Al_2O_3$  particles (I).

## CONCLUSIONS

1. The deformation banded structure appears to be in the extrusion direction may be due to the orientation of  $Al_2O_3$  particles along with the thermal mismatch between  $Al_2O_3$  particles and Al 2014 matrix alloy during hot extrusion process.
2. The composite with a higher value of sonic modulus will have a lower value of impact strength. Higher volume percent of reinforcement has led to the lower absorption of impact energy.
3. Improvement of sonic modulus properties is related to the volume percent of reinforcement. The content of reinforcement should be controlled to the acceptable limit to ensure that it can maintain the impact strength and optimise the toughness properties of the composites.
4. The fracture mechanism is indicated by matrix ductile rupture and decohesion at the particle-matrix interface in Composite 1 whereas matrix brittle rupture by particle fracture is found in Composite 2.

## ACKNOWLEDGEMENT

The authors are grateful to MOSTE for the financial support.

## REFERENCES

1. D.J. Lloyd, (1994). Particle Reinforced Aluminium and Magnesium Matrix Composites, *International Materials Reviews*, 39(1): 1-23.
2. Y. Sahin, (2003). Preparation and Some Properties of SiC Particle Reinforced Aluminium Alloy Composites, *Materials and Design*, 24: 671–679.
3. H.X. Peng, Z. Fan, D.S. Mudher and J.R.G. Evans, (2002). Microstructures and Mechanical Properties of Engineered Short Fibre Reinforced Aluminium Matrix Composites, *Materials Science and Engineering*, A335: 207–216.
4. K.R. Ahmad, J.B. Shamsul, L.B. Hussain and Z.A. Ahmad, (2003). Preliminary Study of Aluminium Metal Matrix Composite Reinforced with Alumina Partic Via P/M Route, *Proceedings of International Conference on Recent Advances on Materials, Minerals and Environment*, 391-394.
5. Umit Cocen and Kazim Onel, (2002). Ductility and Strength of Extruded SiCp/ Aluminium-Alloy Composites, *Composites Science and Technology*, 62: 275–282.
6. T.J .A. Doel and P. Bowen, (1996). Tensile Properties of Particulate-Reinforced Metal Matrix Composites, *Composites*, 27A: 655-665.
7. F.J. Humphreys, (1991). The Thermomechanical Processing of Al-SiC Particulate Composites, *Materials Science and Engineering*, A135: 267-273.

8. B. Derby, (1995). Microstructure and Fracture Behaviour of Particle-Reinforced Metal-Matrix Composites, *Journal of Microscopy*, 177: 357-368.
9. J.C. Malas, S. Venugopal and T. Seshacharyulu, (2004). Effect of Microstructural Complexity on the Hot Deformation Behaviour of Aluminium Alloy 2024, *Materials Science and Engineering*, A368: 41-47.
10. Tongxiang Fan, Di Zhang, Guang Yang, Toshiya Shibayanagi and Massaki Naka, (2003). Fabrication of In Situ  $Al_2O_3/Al$  Composite via Remelting, *Journal of Materials Processing Technology*, 142: 556-561.
11. Miserez, A. Rossoll and A. Mortensen, (2004). Fracture of Aluminium Reinforced with Densely Packed Ceramic Particles: Link Between The Local and The Total Work of Fracture, *Acta Materialia*, 52: 1337-1351.
12. J.I Song and K.S. Han, (1997). Fracture Toughness Evaluation of Hybrid Metal Matrix Composites, *Proceedings of 11<sup>th</sup> International Conference on Composite Materials (ICCM-11)*, 3: 327-336.
13. Kohyama, N. Niwa and S. Sato, (1993). In-Situ Observation of Deformation and Fracture Process for Metal Matrix Composites under SEM and SAM, *Key Engineering Materials*, 79-90: 279-294.
14. Wenlong Zhang, Mingyuan Gu, Jiayi Chen, Zhengan Wu, Fan Zhang and Herve E. Deve, (2003). Tensile and Fatigue Response of Alumina-Fiber-Reinforced Aluminium Matrix Composite, *Materials Science and Engineering*, A341: 9-17.
15. Julie Champlin, J. Zakrajsek, T.S. Srivatsan, P.C. Lam and M. Manoharan, (1999). Influence of Notch Severity on the Impact Fracture Behavior of Aluminum Alloy 7055, *Materials and Design*, 20: 331-341.
16. W. M. Lima, F. J. Velasco, J. Abenojar and J. M. Torralba, (2003), Numerical Approach for Estimating the Elastic Modulus in MMCs as a Function of Sintering Temperature, *Journal of Materials Processing Technology*, 143-144; 698-702.
17. S. Biwa and T. Shibata, (2000). Elastic and Ultrasonic Properties of a Unidirectional Composite with Partially Debonded Fibres: Numerical Analysis for Longitudinal Shear Modes, *Composites Science and Technology*, 60; 83-93.
18. Jacques E. Schoutens, (1985). The Elastic and Compressive Properties of Hybrid Metal Matrix Composites/Hexagonal Prismatic Cellular Solids, *Composite Structures*, 4; 267-291.
19. Cemal Aksel and Frank L. Riley, (2003). Young's Modulus Measurements of Magnesia-Spinel Composites using Load-Deflection Curves, Sonic Modulus, Strain Gauges and Rayleigh Waves, *Journal of the European Ceramic Society*, 23: 3089-3096.



20. T. Christman and S. Suresh, (1988). Microstructural Development in an Aluminum Alloy-SiC Whisker Composite, *Acta Metallurgica*, 36; 1691-1704
21. Ozdmir U, Cocen U and Onel K.(2000). The Effect of Forging on the Properties of Particulate SiC Reinforced Aluminium Alloy-Composites, *Composites Science and Technology*, 60: 411-419.